757 NLF GLOVE FLIGHT TEST RESULTS

L. J. Runyan, G. W. Bielak, R. Behbehani,
A. W. Chen, and R. A. Rozendaal
Boeing Commercial Airplane Company
Seattle, Washington

OBJECTIVES AND APPROACH

A major concern in the application of a laminar flow wing design to commercial transports is whether laminar flow can be sustained in the presence of the noise environment due to wing-mounted turbofan engines. To investigate this issue, a flight test program was conducted by Boeing under contract to NASA Langley using the Boeing 757 flight research airplane with a portion of the wing modified to obtain natural laminar flow (Refs. 1 and 2).

Prior to this flight-test program, there were no extensive measurements of the noise field on the wing of a commercial transport with wing-mounted high-bypass-ratio engines. There also were no flight measurements of the effect of such a noise field on laminar boundary-layer transition. Therefore, the flight test had two primary objectives. The first was to measure the noise levels on the upper and lower surface of the wing for a range of flight conditions. The second was to investigate the effect of engine noise on laminar boundary-layer transition. In order to achieve these objectives, the wing was instrumented with an array of microphones, and a Natural Laminar-Flow (NLF) glove was installed on the right hand wing just outboard of the nacelle. The noise field on the wing and transition location on the glove were then measured as a function of the engine power setting at a given flight condition. (Figure 1).

(NASA Contract NAS1-15325)

Objectives

- **Define noise environment on wing**
- **Investigate effect of engine noise on laminar boundary layer transition**

Approach

- **Install NLF glove outboard of engine**
- **Measure noise field and transition location as function of engine power**

Figure 1

NATURAL LAMINAR FLOW GLOVE INSTALLATION

The objective of the glove design was to obtain enough natural laminar flow to allow the effect of engine noise on the extent of laminar flow to be observed. The extent of natural laminar flow that is obtained with a given pressure distribution is a strong function of leading edge sweep. Lower leading edge sweep results in longer laminar runs. However, lower leading edge sweep has some adverse effects. The bending load due to the overhang increases with decreasing leading edge sweep. The asymmetry of the airplane also increases, which results in possible reduction of the flight envelope. The final choice of the leading edge sweep was 21 deg, which limited the airplane to 2.0-g operations.

The glove location was chosen to be immediately outboard of the No. 2 engine at slat No. 7. This location gives the glove maximum engine noise exposure. The glove was designed with the constraint that it have straight spanlines within the prime test region in order to facilitate its manufacture. It also was designed with the constraint that it match the existing wing at x/c = 0.35 in order to minimize the size of the glove.

Because the glove was considered to be a relatively small departure from the existing 757 wing, for which both wind tunnel and flight data are available, no wind tunnel testing was considered necessary to substantiate the aerodynamic design. The availability of accurate transonic aerodynamic codes was also a factor in the decision to dispense with testing. (Figure 2).

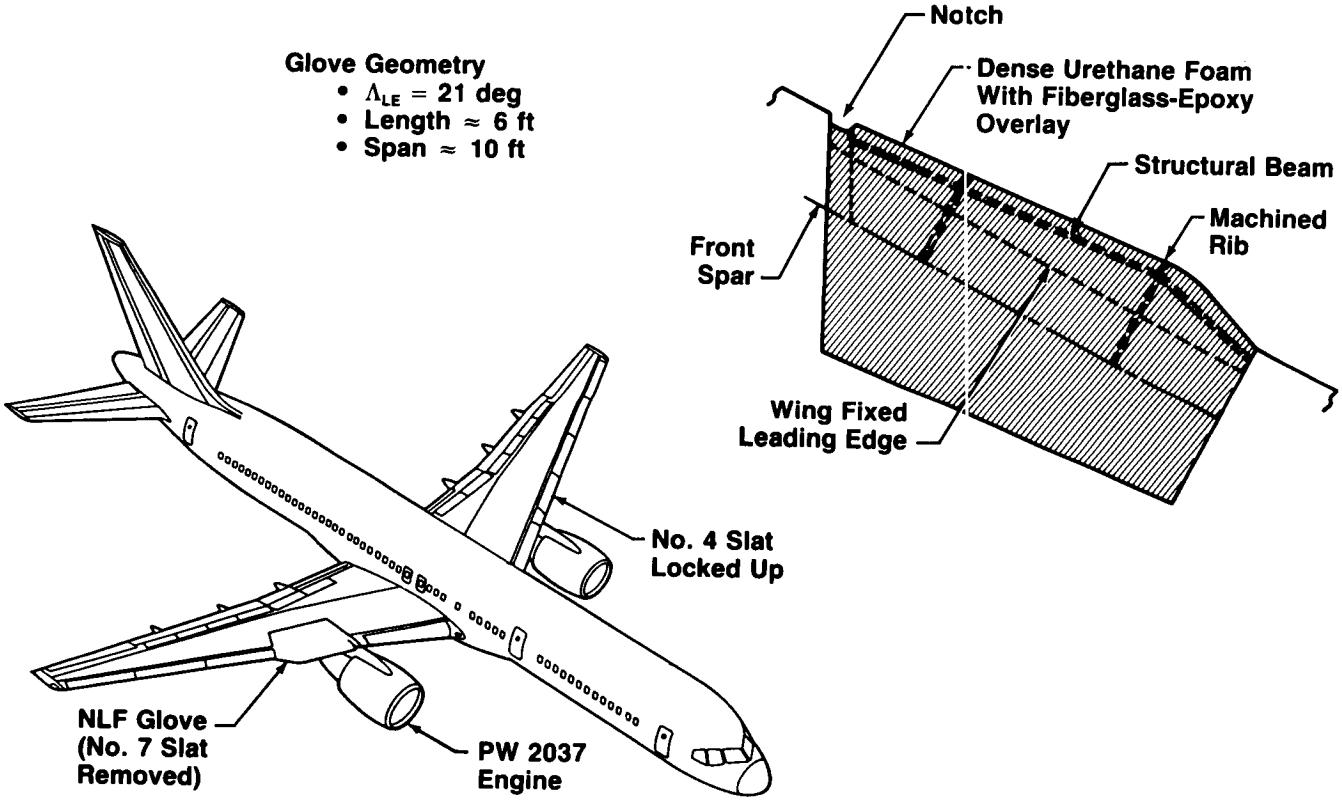

Figure 2

ACOUSTIC INSTRUMENTATION

Eight microphones were mounted on each surface of the wing. One additional microphone was mounted just above the attachment line near the outer edge of the glove. On the forward part of the wing where the boundary layer is thin, the transducers were bonded directly to the wing surface and faired smoothly to the surface using Magic Bond. Each surface-mounted transducer was modified by inserting a 0.016-in wire in the unit's vent tube to provide desired response characteristics. The microphones located further back on the wing were mounted on a probe. The probe height above the wing surface was chosen so that the microphone would be slightly above the boundary layer as calculated for the glove design condition (M = 0.80, altitude = 40,000 ft). The vent tube of each of the probe-mounted transducers was modified by inserting a 0.008-in wire to provide satisfactory response characteristics.

The microphone locations were chosen to survey the entire wing with a limited number of transducers. It was also desired to use a denser distribution of microphones in the NLF glove region for the investigation of sound effects on laminar flow. The microphone placement on the glove recognized that the microphones would trip the laminar boundary layer. Their locations were chosen so that the turbulent wedge emanating from them would not interfere with any of the hot films. (**Figure** 3).

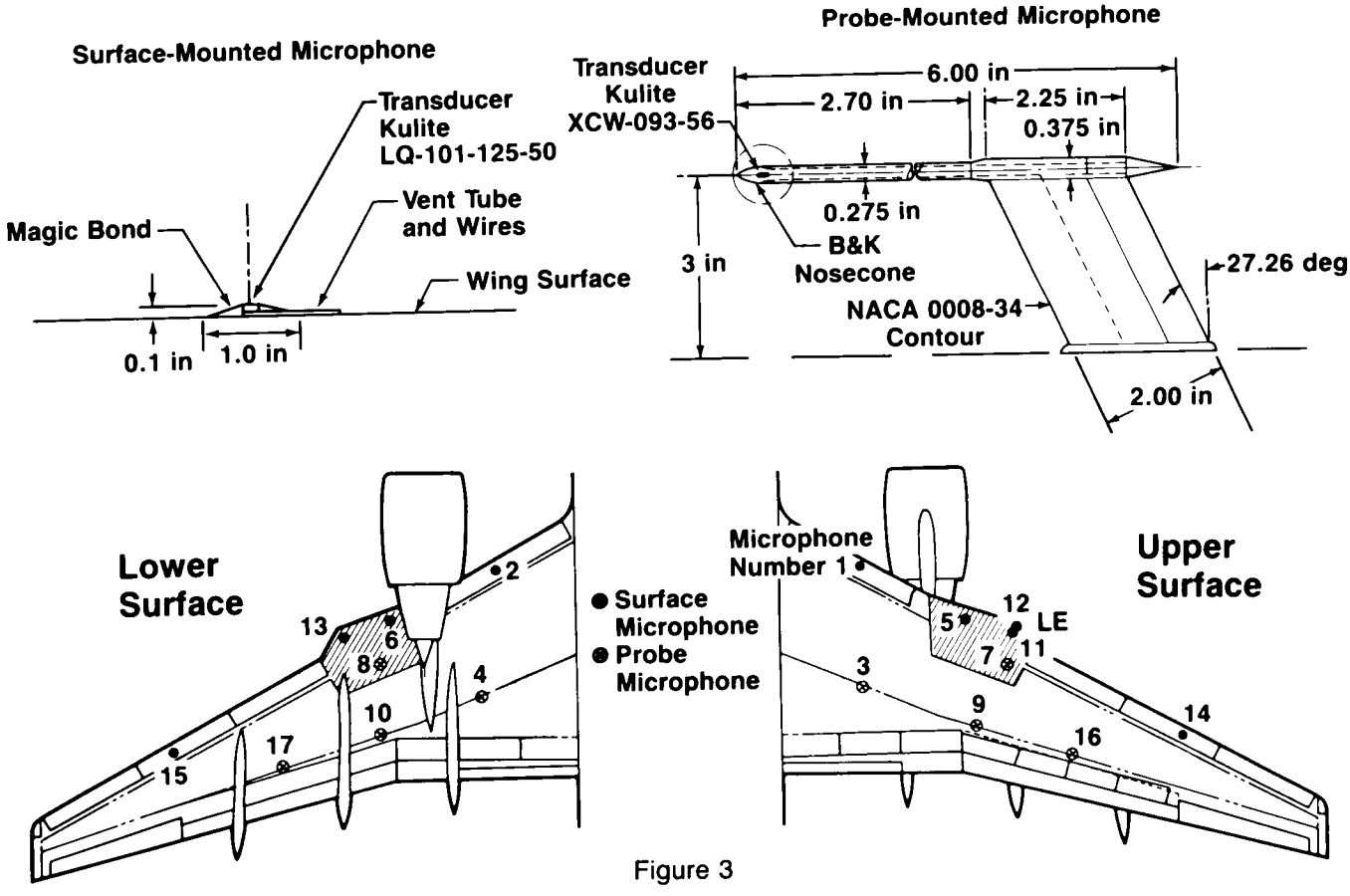

Figure 3

NLF GLOVE INSTRUMENTATION

In addition to the noise-measuring instruments, glove pressure distributions were measured with separate upper and lower surface "strip-a-tube" belts, and the state of the boundary layer was determined by surface hot-film sensors. Two separate pressure belts were used for each glove surface so there would be no chance of contaminating the attachment line flow with a belt wrapped around the leading edge. The pressure belts were carefully faired to the glove surface to minimize the effect of their presence on the measured pressures. The number of available data channels limited the pressure measurements to one section at a time. Therefore, only the pressure belts at the inboard section were used for the first two flights, and only the outboard belts were used for the last two flights. By closely matching the test conditions, measurements from the two sets of flights with different instrumentation layouts could be combined.

The ten hot-film sensors installed on each surface of the glove were staggered 15 deg from a streamwise line so the disturbances created by upstream sensors would not affect the response of downstream sensors. The choice of this angle was based, in part, on transonic analyses that determined the streamline pattern on the glove. On the first two flights the films were placed in a long row to get an accurate chordwise determination of the transition point near the middle of the glove. For the last two flights the sensors were repositioned based on results from the first flights, so the spanwise extent of laminar flow could be determined. (Figure 4).

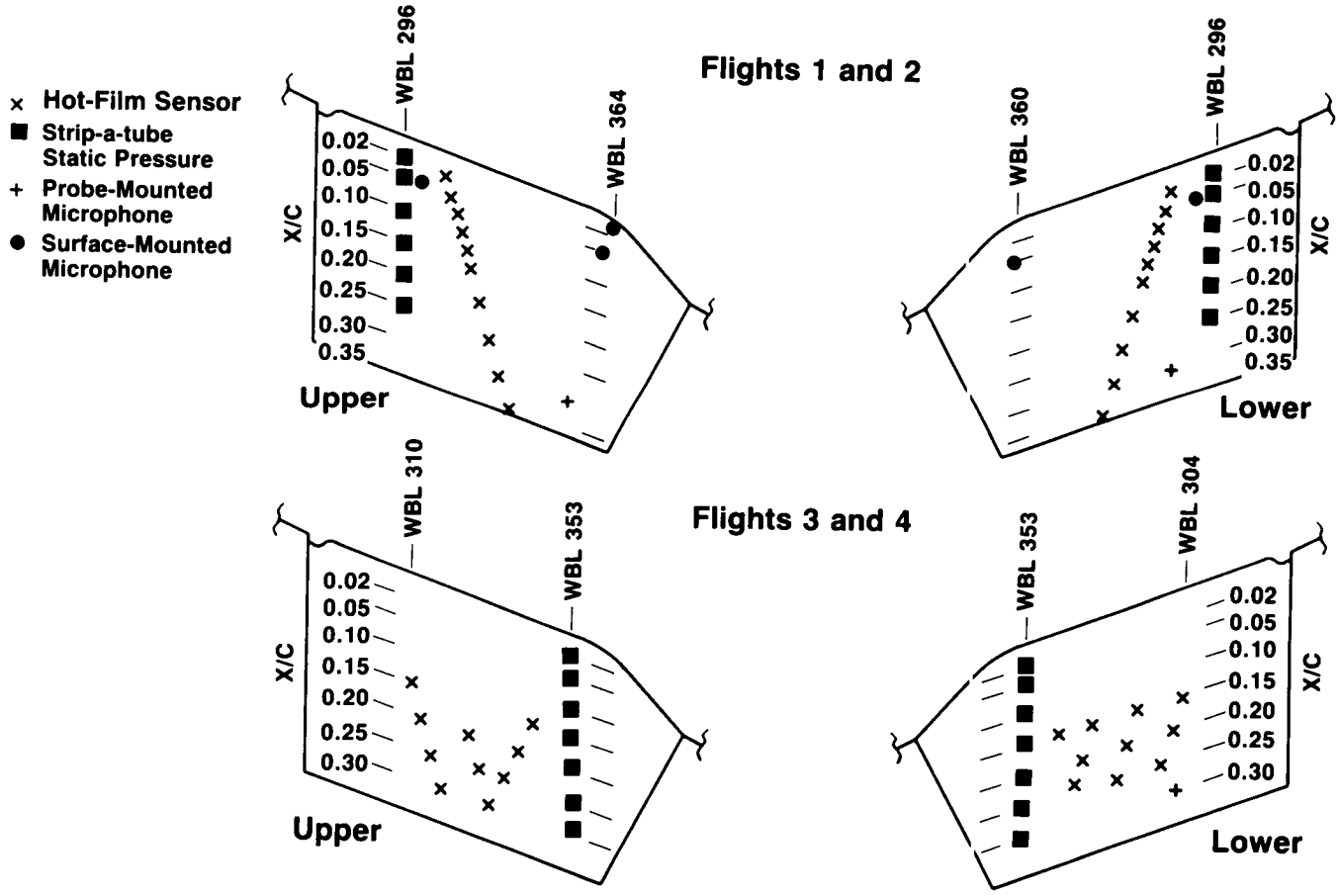

Figure 4

TRANSITION SENSING SYSTEM

The hot-film sensors used for this test were 50-Ohm nickel gages made by Micromeasurement. The electronics that controlled the gages was designed and fabricated at Boeing, and maintained the gages at a constant voltage. The fluctuating current signal from each gage was converted to a voltage and recorded on magnetic tape during each test point interval and also displayed continuously on oscilloscopes. The rms value from each hot film was also recorded.

The oscilloscope displays were used by the test engineer on the flights to determine the boundary-layer state in real time at each of the hot-film locations. The traces exhibited by the hot films fell into four quite distinct categories. A laminar trace was nearly flat with an rms signal value of about 10 mV. The next development was an intermittent signal burst superimposed on the laminar signal. This was interpreted as being discrete bursts of turbulence moving past the gage. These intermittent bursts eventually replaced the laminar signal as the boundary layer moved into its transitional phase. The transitional signal had rms values of several hundred millivolts. As the boundary layer became fully turbulent, the signal settled down from the wildly fluctuating transitional trace to a steady state fluctuation having an rms value around 50 mV. (Figure 5).

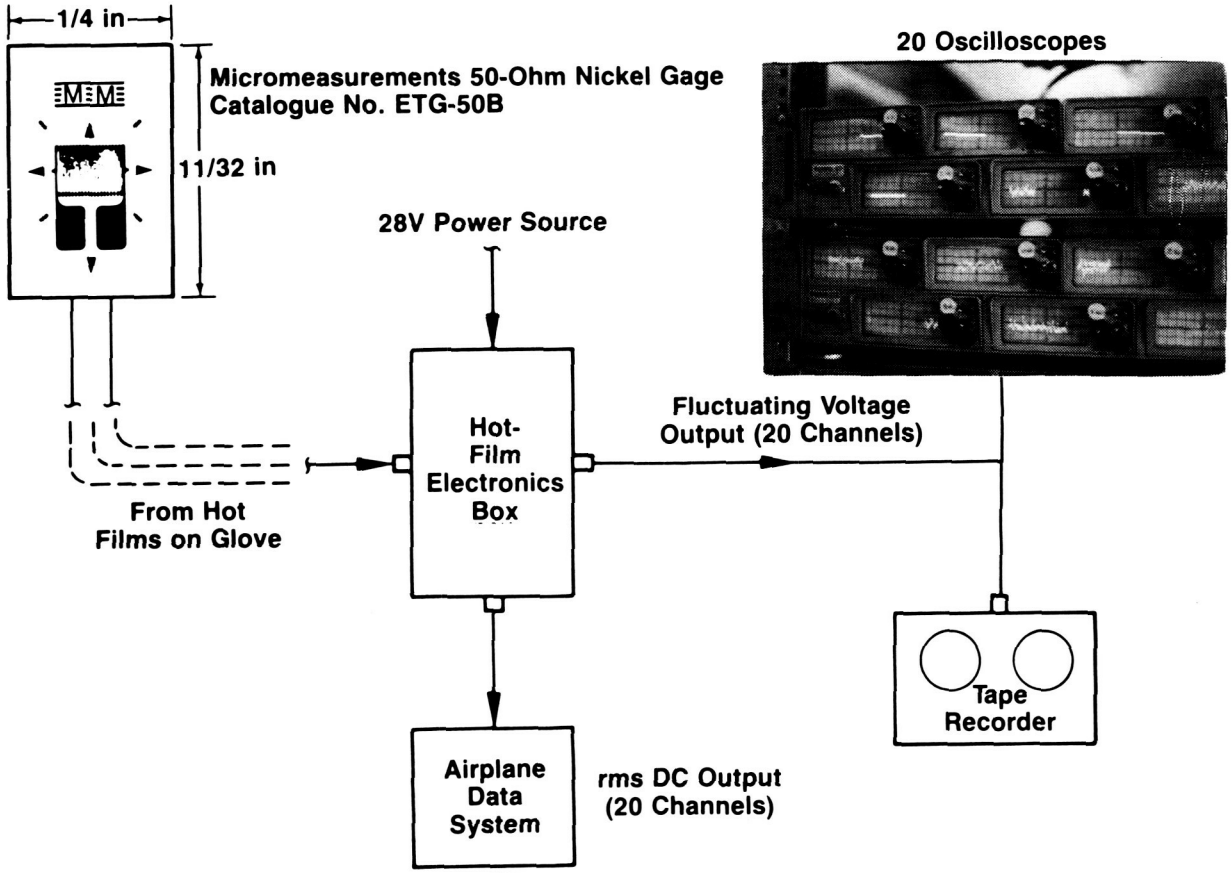

Figure 5

INSECT PROTECTION COVER

Because the glove was flight tested in June, it was necessary to protect the test area from insect impingement that would result in contamination of the laminar flow. The technique used was similar to that used successfully in the King Cobra flight-test program (Ref. 3). The leading-edge area was covered with paper during takeoff and climb. The paper used was similar to butcher paper in strength and thickness, with a thin film of wax on the side next to the glove surface. To remove the paper, a heavy nylon rip cord was led under the leading edge of the cover to its outboard end and then back through a small paper envelope attached to the outside leading edge of the cover. The cord was attached to the cover at its inboard end and was protected from the airflow by the envelope. The cord was run into the cabin through a 0.25-in copper tube that was secured to the wing and body surfaces. After the airplane climbed above 5000 ft, the cord was pulled, ripping the paper into two halves that flew away. The ripping mechanism did not work as planned on the first two flights because of initial problems with the routing of the copper tube and the strength of the rip chord. "Roller-coaster" type maneuvers had to be used to shake off the paper. On flight 3, the ripping mechanism worked as planned. On all 3 of those flights there was no evidence of insect contamination, indicating that the cover did provide the desired protection. (Figure 6).

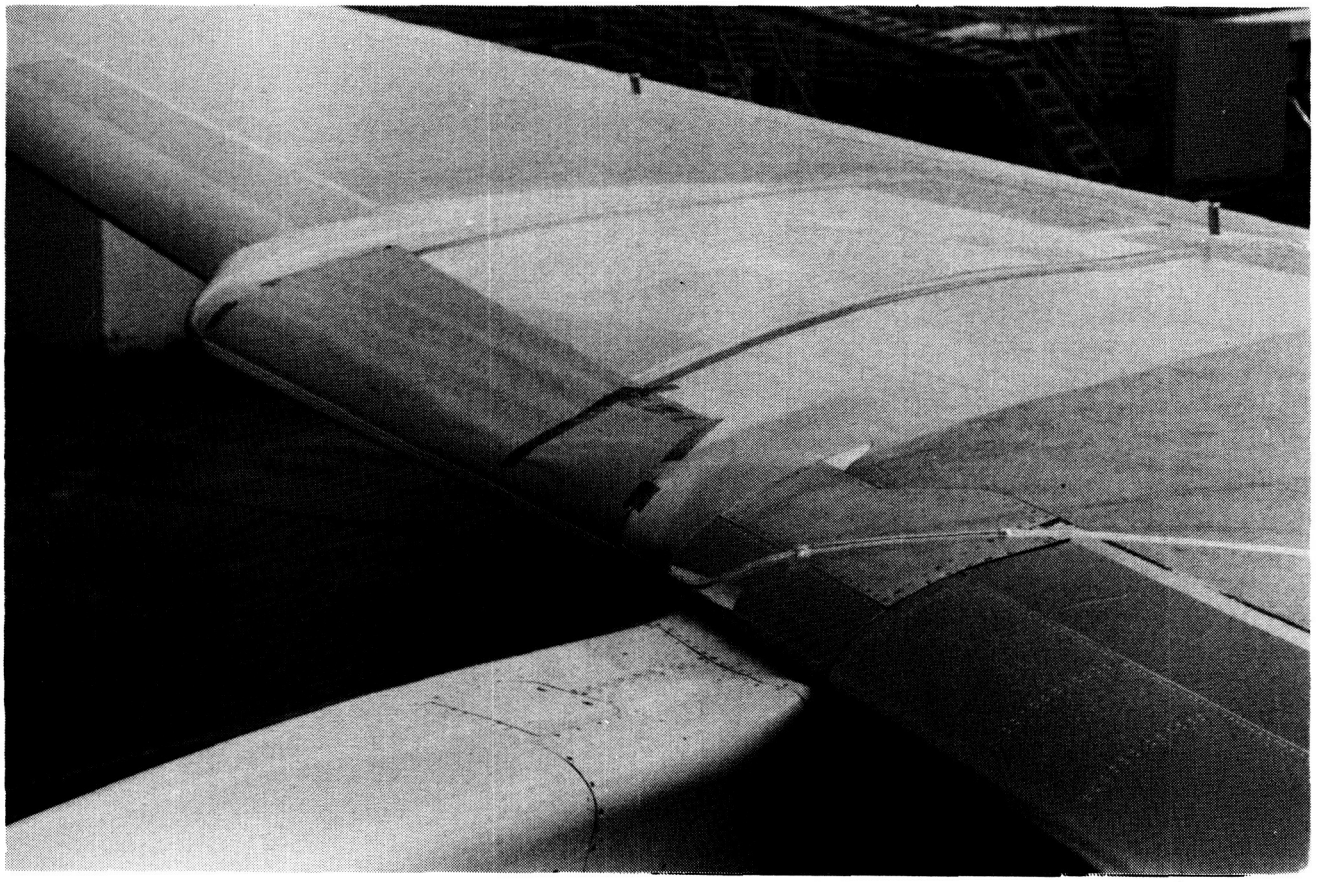

Figure 6

INSECT IMPINGEMENT ON UNPROTECTED GLOVE

The glove was not protected during flight 4 since the primary purpose of that flight was to obtain pressure data. Laminar flow sensor data taken on the flight indicated a loss of laminar flow in some areas of the glove relative to the flight 3 results. It was suspected that this was due to insect contamination, although this could not be visually confirmed in flight. After landing, an inspection of the glove leading edge showed that seven insects had hit the glove in the vicinity of the attachment line. It is not known how many of these were picked up during takeoff and climbout. However, this evidence, together with the reduced extent of laminar flow in some areas of the glove, indicates that the cover served its essential purpose on the three flights for which it was used. (Figure 7).

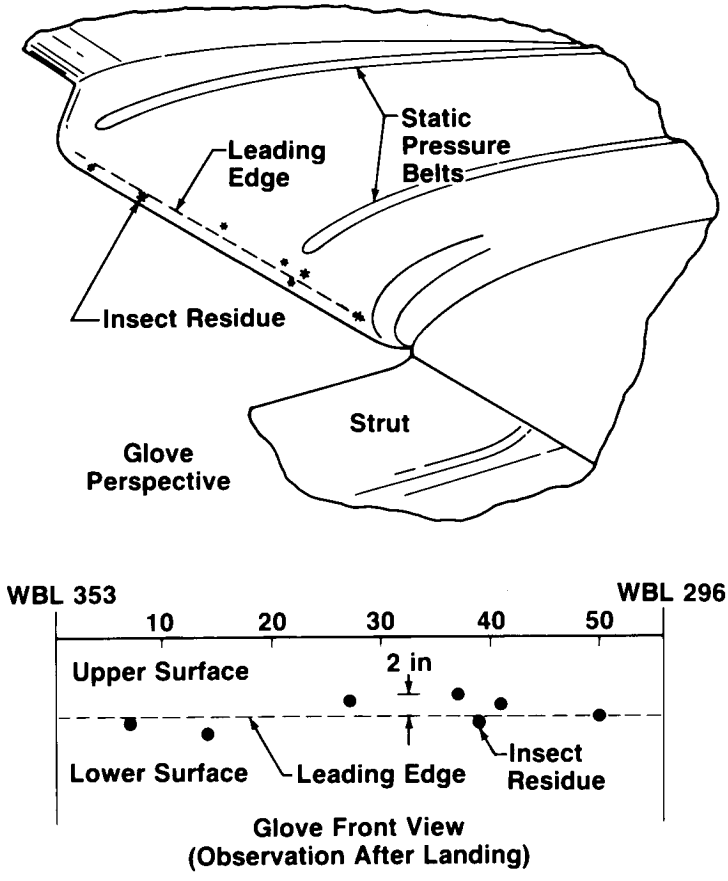

Figure 7

MACH ALTITUDE CONDITIONS TESTED

The design point of the NLF glove was M = 0.8 and an altitude of 40,000 ft At this condition it was expected that a significant extent of laminar flow would be achieved on the upper and lower surface of the glove simultaneously. However, it was also expected that the condition for maximum extent of laminar flow on the upper surface would be obtained at a condition different from that of the lower surface, both of which would differ from the design condition. Furthermore, it was necessary to study the effects of Reynolds number, Mach number, lift coefficient, and sideslip on the extent of laminar flow. The effect of altitude and Mach number on the measured noise levels was also desired. Therefore, a wide range of Mach-altitude conditions were tested, as shown in Figure 8. The Mach numbers tested ranged from 0.63 to 0.83, and the altitudes ranged from 25,000 ft to 41,000 ft. The most important Mach numbers were 0.8 and 0.7, and the most important altitudes were 39,000 ft and 35,000 ft.

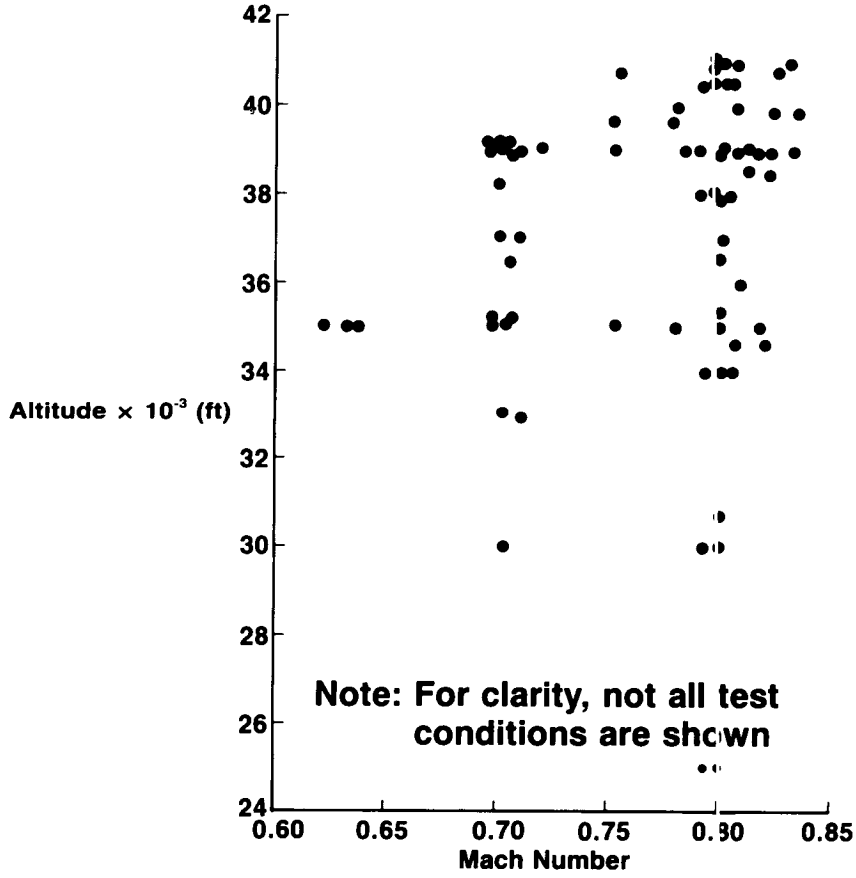

Figure 8

OASPL DISTRIBUTION ON 757 WING

Figure 9 shows the overall sound pressure level (OASPL) distribution measured on the wing for a cruise engine power setting at an airplane Mach number of 0.81 and an altitude of 39,000 ft. The upper surface noise levels range from 111 dB to 131 dB. The lower surface noise levels range from 121 dB to 136 dB. This data is presented to give an overview of the noise levels measured. The flight-test program resulted in a large data base of this type of noise data for a large range of flight conditions and engine power settings. In addition, the spectral characteristics of the noise at each microphone location were measured.

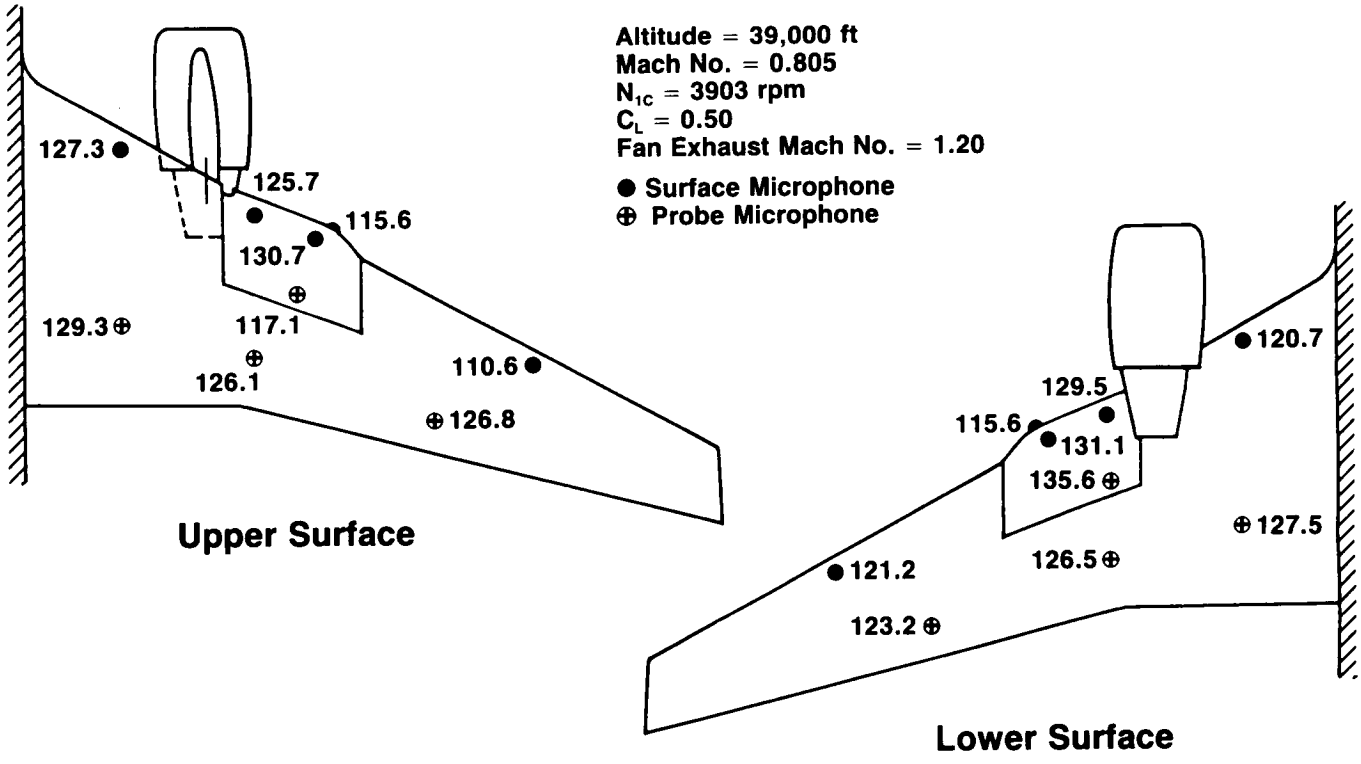

Figure 9

NORMALIZED OASPL VERSUS FAN MACH NUMBER
(Forward Surface Microphones)

Figure 10 shows the relationship of the noise overall sound pressure level (OASPL) to engine power condition (M_{FAN} = fan exhaust jet fully expanded Mach number) for one forward surface microphone on the upper surface and one on the lower surface. Curves are shown for airplane Mach numbers from $M_{AP} \simeq 0.63$ to $M_{AP} \simeq 0.82$. A clear engine power dependence, with very little airplane Mach number dependence, is seen for the lower surface microphone. This engine power dependence indicates a dominance of engine noise. The point labeled "nacelle spillage" is believed to result from turbulent airflow from the engine nacelle impinging on the wing. For this condition the engine was at idle with the airplane in a slight dive to maintain speed.

The upper surface microphone generally does not show an engine power dependence but does show an airplane Mach number dependence. Except for the "nacelle spillage" point the highest noise levels were observed for the lowest airplane speed condition. The engine noise is apparently shielded from the microphone by the wing surface. The pressure fluctuations that the microphone is responding to are probably related to turbulent flow over the microphone.

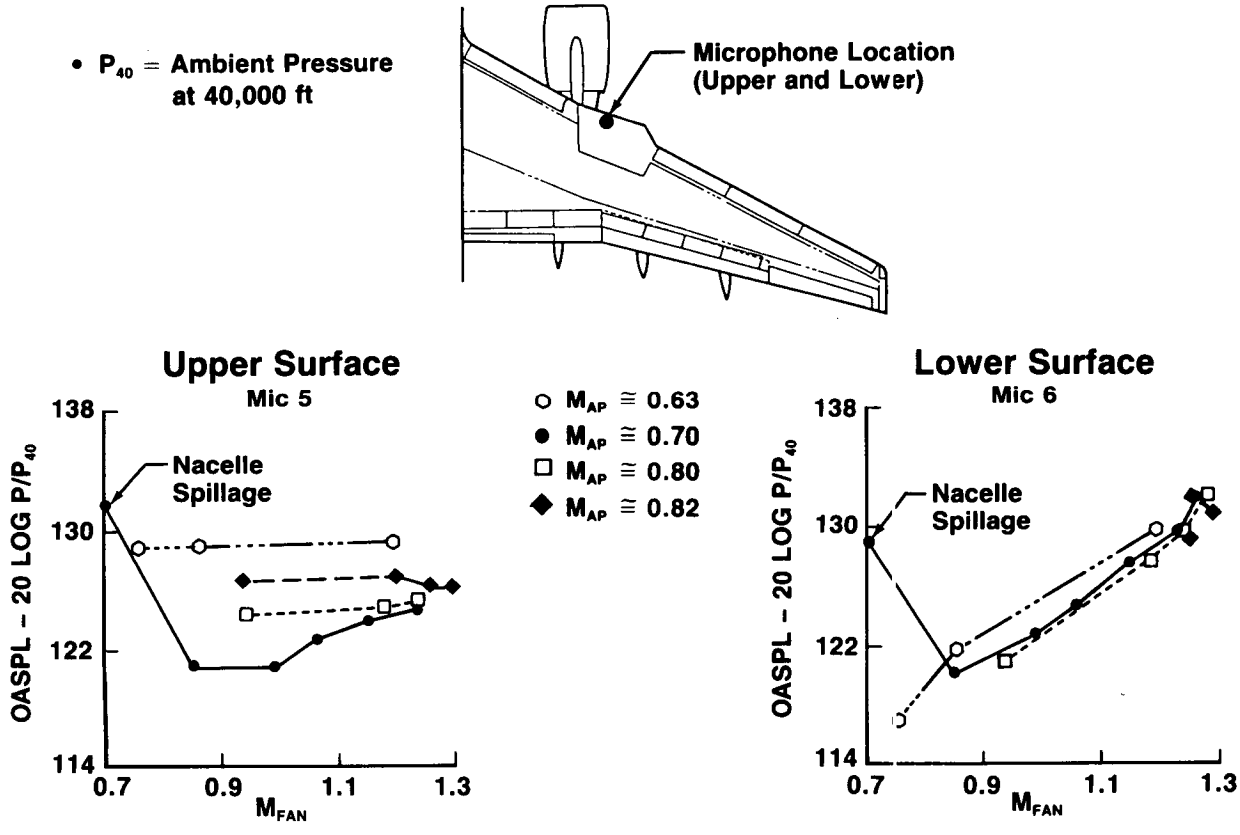

Figure 10

NOISE CHARACTERISTICS AT NLF GLOVE UPPER SURFACE LEADING EDGE MICROPHONE

For the higher Mach number conditions ($M_{AP} \approx 0.8$) the boundary layer on the upper glove surface was found to be laminar back to 20% to 30% chord. The high noise levels measured by microphone 5 therefore suggest that the microphone or microphone fairing was causing the local boundary layer to become turbulent near the microphone. The noise level initially decreases as C_L increases. The airplane mach number decreases for the higher C_Ls so that a M_{AP} dependence is possibly influencing the data to some degree. For $C_L \geq 0.62$ the noise level begins to increase with C_L. For these points the hot-film data indicated that the laminar boundary layer transition point was very close to the glove leading edge. The increased noise level is probably related to this transition. It is interesting to note that the one-third octave spectrum shape for the low Mach number/high C_L points at microphone 5 (lower left of Figure 11) is quite different from the higher Mach number cases (lower right of Figure 11). It appears that the boundary-layer transition resulted in lower frequency noise than that due to the microphone-generated turbulence.

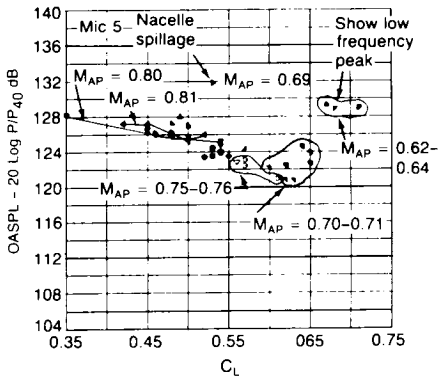

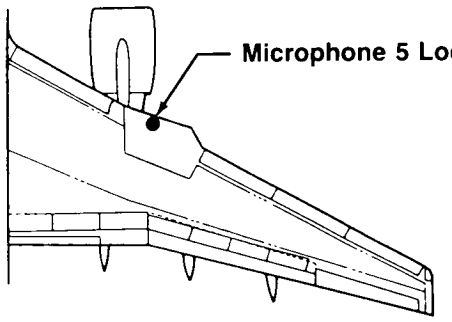

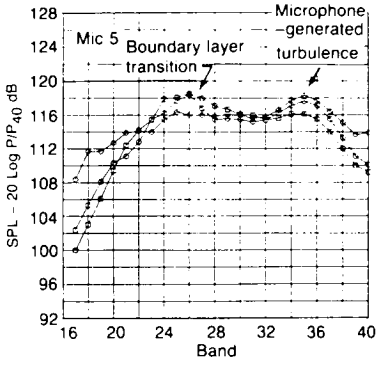

Cond.		M_{AP}	M_{FAN}	C_L
221	○	0.63	0.76	0.68
220	□	0.62	0.86	0.71
219	◇	0.64	1.19	0.67

Hot Film rms Voltage ~ V

Cond.	x/c 5%	x/c 7.5%
221	0.032	0.039
220	0.033	0.041
219	0.036	0.041

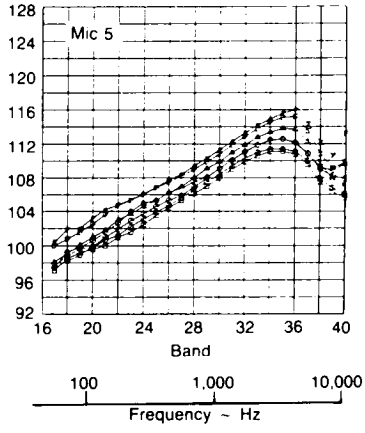

Cond.		M_{AP}	M_{FAN}	C_L
236	○	0.71	0.85	0.62
237	□	0.71	0.99	0.63
218	◇	0.70	1.05	0.62
217	◇	0.71	1.06	0.60
233	△	0.70	1.06	0.65
232	▽	0.70	1.15	0.65
231	▽	0.70	1.23	0.64

Hot Film rms Voltage ~ V

Cond.	x/c 5%	x/c 7.5%
236	0.006	0.089
237	0.005	0.087
218	0.006	0.030
217	0.010	0.034
233	0.006	0.033
232	0.006	0.034
231	0.005	0.038

Figure 11

ENGINE NOISE SPECTRA ON LOWER WING SURFACE

Figure 12 shows narrow band spectra for two microphones on the lower surface of the wing. Measurements for a range of engine power conditions at an airplane Mach number of approximately 0.8 and an altitude of approximately 40,500 ft are shown. Tones identifed as originating from the engine fan (1F, 2F, 3F and 4F—fan blade passing harmonics) and turbine (T4 and T5—fourth and fifth stage low pressure turbine blade passing frequency tones) are clearly seen. Other tones and higher frequency broadband maxima are not identifiable as engine related. The low frequency (500 Hz-1000 Hz) broadband noise peak that increases with engine power (M_{FAN}) is believed to be due to the interaction of jet exhaust turbulence and shocks.

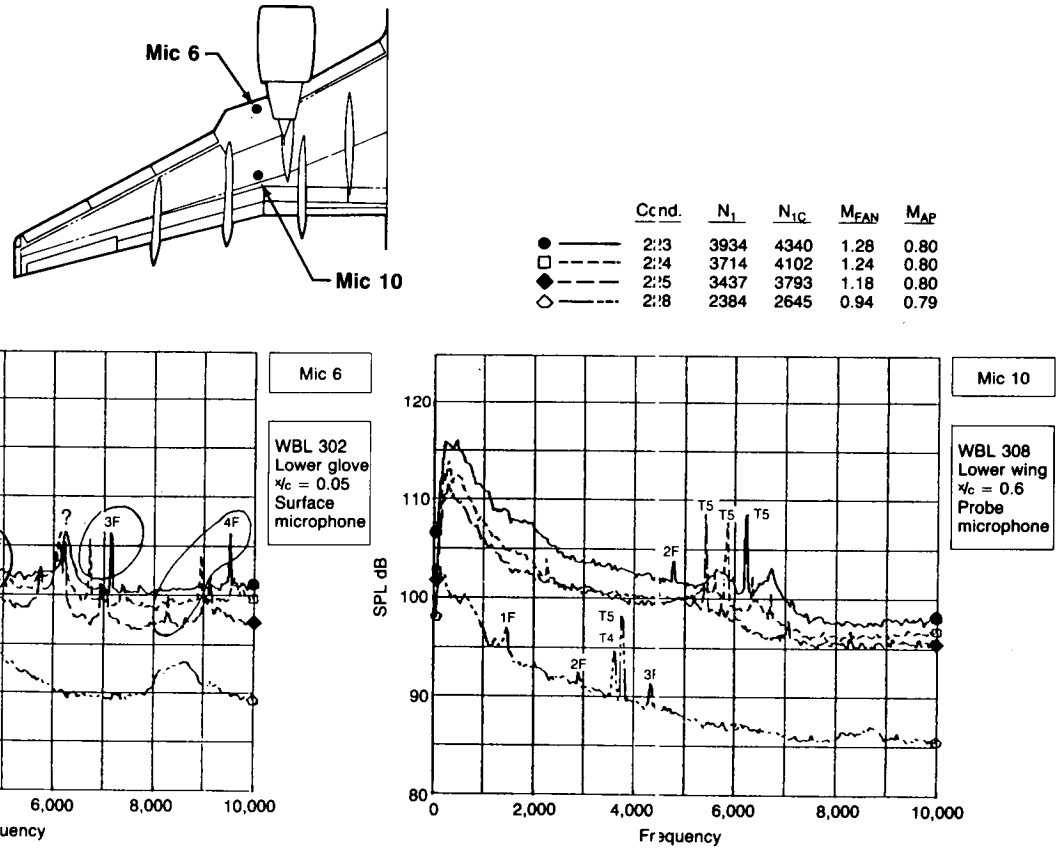

Figure 12

NORMALIZED OASPL VERSUS FAN MACH NUMBER
(Aft Probe Microphones)

The aft probe microphones indicate, as did the forward surface microphones, that there is very little engine power dependence of the noise levels on the upper surface, but a strong engine power dependence on the lower surface. Also, the upper surface data shows a strong airplane Mach number dependence, while the lower surface data shows very little airplane Mach number dependence. (Figure 13).

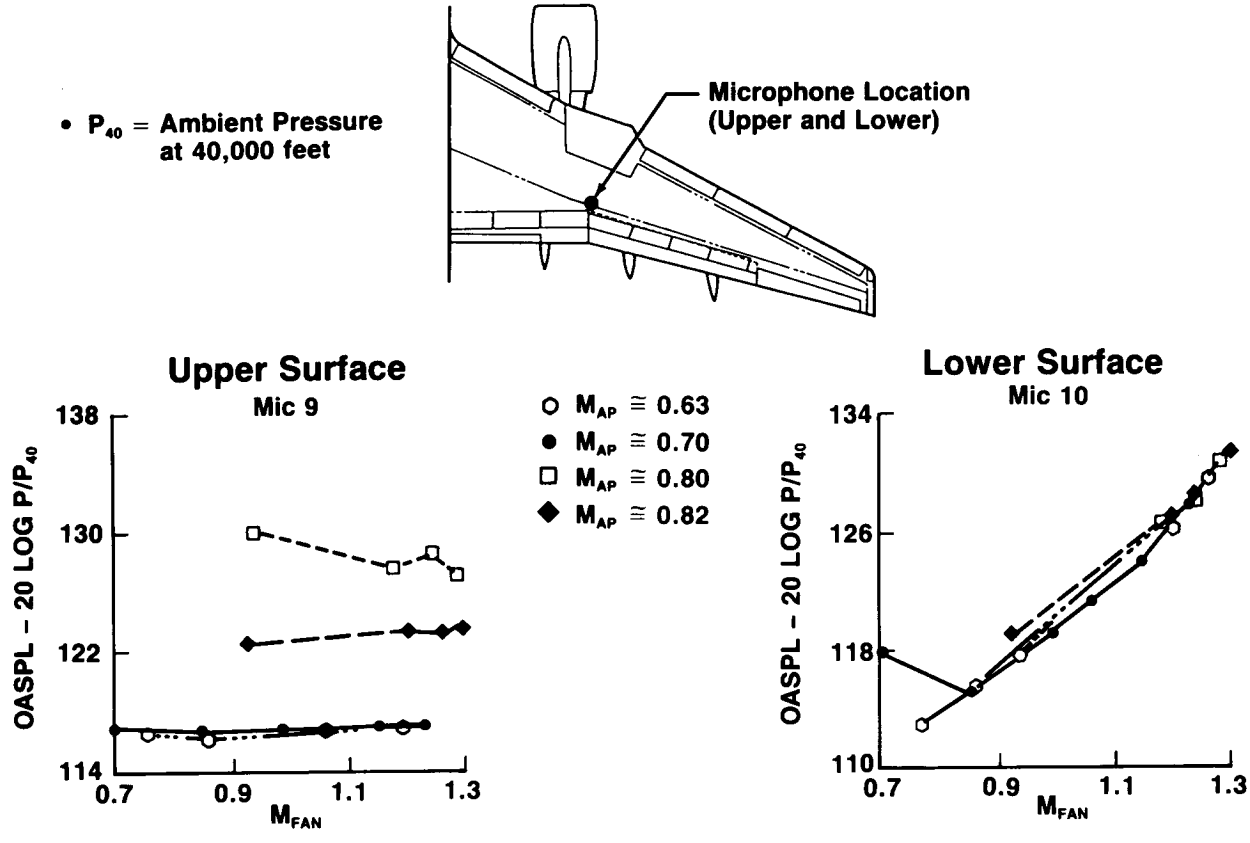

Figure 13

EFFECT OF SHOCK LOCATION ON UPPER SURFACE NOISE

The effect of the wing shock location on the upper wing microphone noise spectra measurements is shown in Figure 14. As the airplane Mach number is increased from 0.70 to 0.80, the wing shock is shown to move from just forward of microphone 7 to just forward of microphone 9. For both microphones, maximum noise levels are observed when the shock is just forward of the microphone. At microphone 7 the one-third octave spectrum peaks in a much higher frequency range than for microphone 9. This is probably related to the thinner boundary layer thickness at microphone 7. The high noise levels observed may be due to boundary layer turbulence directly or sound generated by the shock wave interacting with the turbulent boundary layer. The increased thickness of the boundary layer behind the shock may have been sufficient to cause high levels of boundary-layer pressure fluctuations at the elevated probe microphone as the shock gets closer and stronger with increasing airplane Mach number.

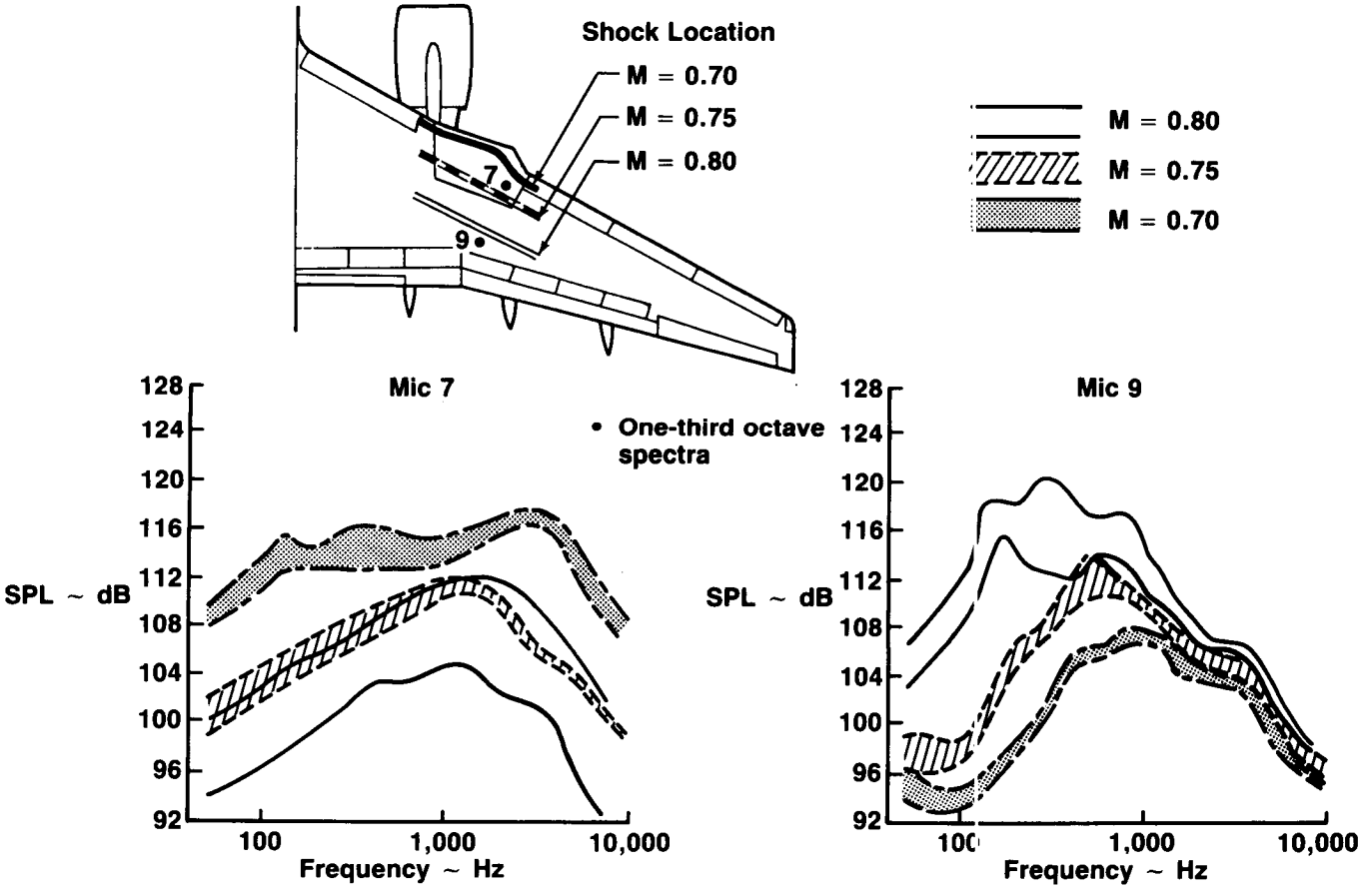

Figure 14

MICROPHONE 10 MEASURED OASPLs VERSUS LOCKHEED PROCEDURE PREDICTIONS

Predictions of the noise measured by the microphones mounted on the lower wing surface were made using near-field engine noise and airframe noise prediction methods incorporated into a computer program by the Lockheed-Georgia Company under contract to NASA. A description of these methods can be found in Reference 4. Predicted noise levels for various engine and airframe noise sources are compared to measured noise levels for microphone 10 in Figure 15. For one plot the predictions were made using the forward motion corrections incorporated into the computer program. High values for the trailing-edge airframe noise component resulted at all microphones with these forward motion corrections. The fan jet shock broadband noise component is seen to be well predicted at the microphone shown using the forward motion corrections. However, for the leading-edge microphones this component over-predicted the data by as much as 40 dB. As a result, predictions were calculated with the forward motion corrections not applied. This resulted in much lower predictions for the trailing-edge noise at all microphones. The fan jet shock broadband noise prediction increased for the aft probe microphones, as shown, and decreased for the forward microphone locations. Overall it is felt that more accurate predictions resulted without the forward motion corrections.

At the higher engine power conditions the predictions indicate that the measured noise is predominately due to the fan jet shock broadband source. The predicted dependence of the noise from this source on fan exhaust Mach number as well as airplane Mach number is consistent with the measurements. For fan exhaust mach numbers less than one, the fan jet shock noise source no longer contributes to the engine noise. The predictions shown indicate a dominance of turbine noise for these conditions, but narrowband data indicates lower frequency broadband noise to be dominant. The prediction method would not give jet mixing predictions for microphones close to the engine but predicted jet mixing results at the other microphones led to the conclusion that jet mixing noise was not an important source. The source of the broadband noise floor at lower engine power settings was not identified.

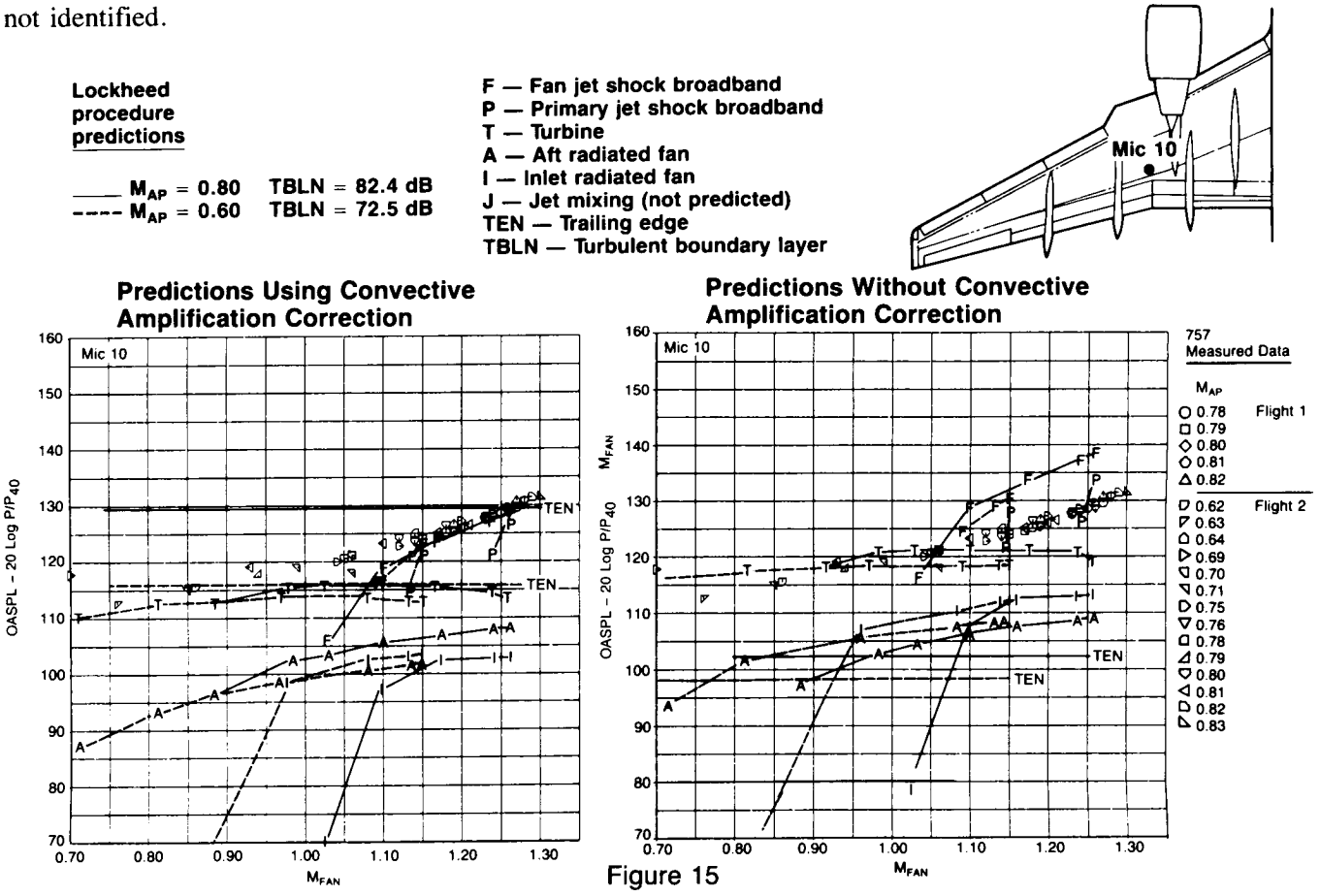

Figure 15

MEASURED EXTENT OF LAMINAR FLOW

The glove design condition was chosen so that a significant extent of laminar flow could be obtained on the upper and lower surface simultaneously. Figure 16 shows that at this condition the upper surface had about 28% chord laminar flow (4.7 ft) in the inboard portion of the test area, while the lower surface had about 18% chord laminar flow (3.0 ft). The decreased extent of laminar flow on the outboard portion of the upper surface was due to a peak in the pressure distribution in that area at about 5% chord. This peak was not predicted by the transonic analysis program used to design the glove. This was probably due to the difficulty of modeling the rapid planform changes occurring at the outboard edge of the glove.

The maximum extent of laminar flow on the upper surface (29% chord) occurred at a high Mach number condition. The extent of laminar flow was only slightly more than at the design condition. The maximum extent of laminar flow on the lower surface (27% chord) occurred at a low Mach, high C_L, high sideslip condition. The high sideslip resulted in an effective sweep reduction that was beneficial in reducing cross-flow instability on the lower surface. High sideslip was less beneficial on the upper surface because it increased the peakedness of the pressure distribution.

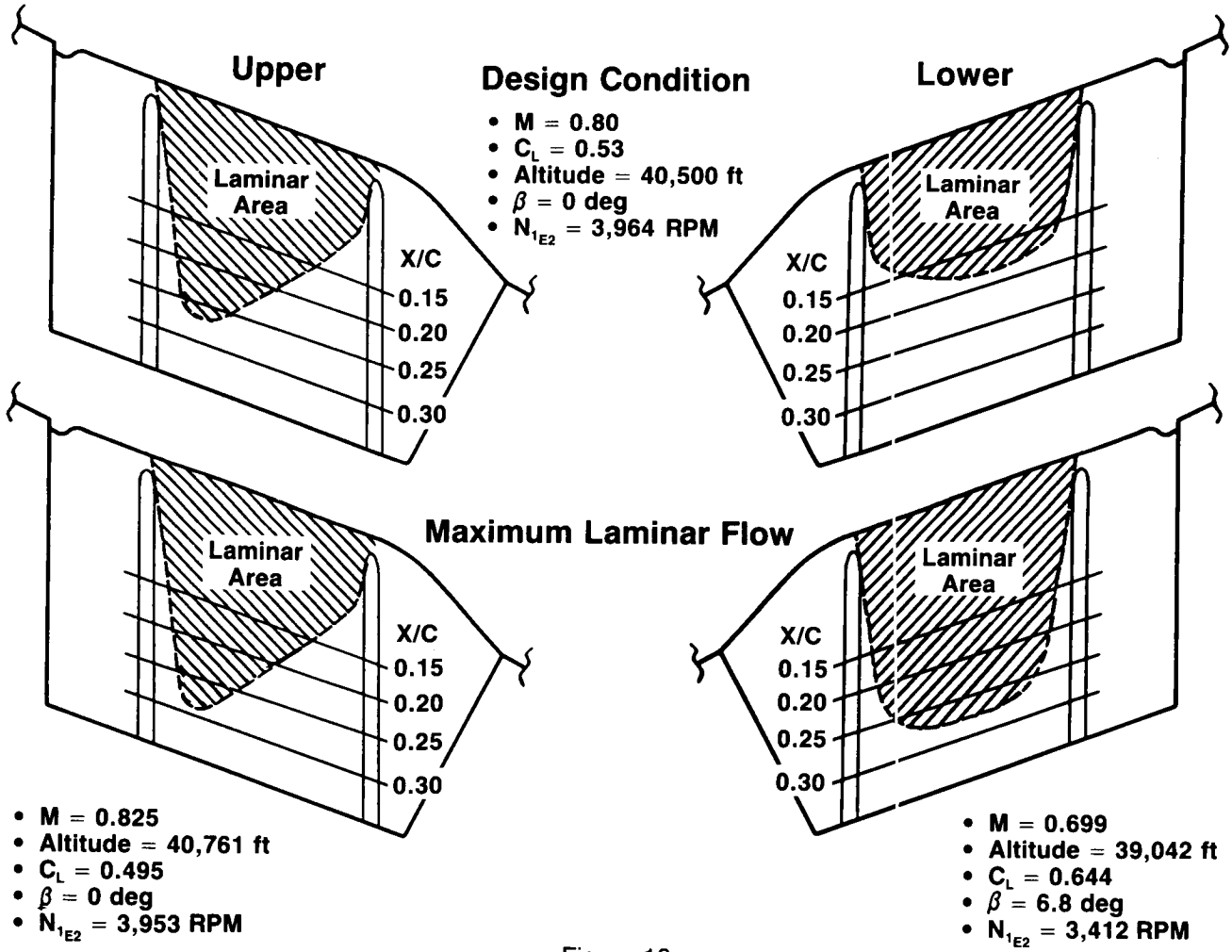

Figure 16

C-3

EFFECT OF LIFT COEFFICIENT AND MACH NUMBER ON EXTENT OF LAMINAR FLOW

As shown in Figure 17, at the design Mach number of 0.8, both the upper surface and the lower surface performed best at high lift coefficients. The decrease in extent of laminar flow at low lift coefficients was probably due to increased cross-flow instability resulting from the decreased flow acceleration near the leading edge at the low lift coefficients. Also, the lower lift coefficients corresponded to lower altitudes and, therefore, higher Reynolds number.

The upper surface extent of laminar flow exhibited a strong Mach number dependency. The greatest extent of laminar flow occurred at the highest Mach number. As the Mach number decreased, a forward pressure peak developed along the entire span of the glove that moved the transition location forward. On the lower surface the greatest extent of laminar flow was obtained at Mach numbers between 0.75 and 0.78. The Mach number dependency on the lower surface was not as strong as on the upper surface.

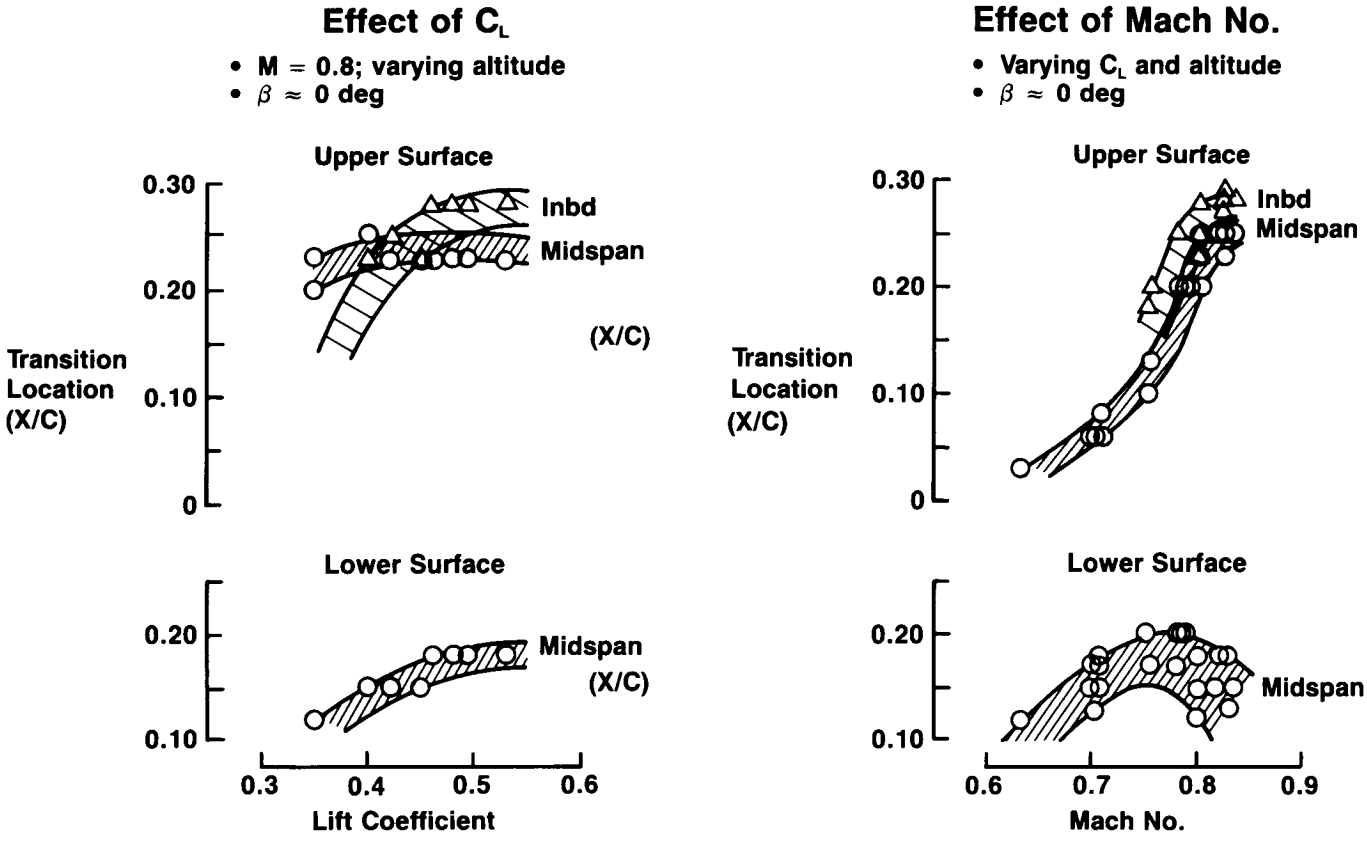

Figure 17

EFFECT OF ENGINE POWER SETTING ON EXTENT OF LAMINAR FLOW

One of the primary objectives of the flight program was to determine the influence of engine noise on transition. As discussed previously, the noise measurements indicated that aerodynamic noise is dominant on the upper surface of the wing. Therefore, it is not surprising that there does not appear to be a clear correlation between the measured upper surface transition location at a given flight condition and the engine power setting, as shown in Figure 18. The M = 0.70, C_L = 0.64 case does show a small forward shift in the transition location at the high power settings. However, as discussed earlier, there does not appear to be any noticeable change in engine noise on the upper surface at this Mach number with changes in engine power setting. Therefore, the small change in extent of laminar flow (the hot film at 7.5% chord went from turbulent to transitional) at this condition may have actually been due to small differences in lift coefficient between the low and high power settings.

The lower surface noise measurements, discussed previously, showed that engine noise is dominant at all flight conditions. As shown in Figure 18, the lower surface transition location does show a greater sensitivity to the engine power setting than was the case for the upper surface. At most flight conditions, there was 2% to 3% less laminar flow at the high power settings than at the low power settings.

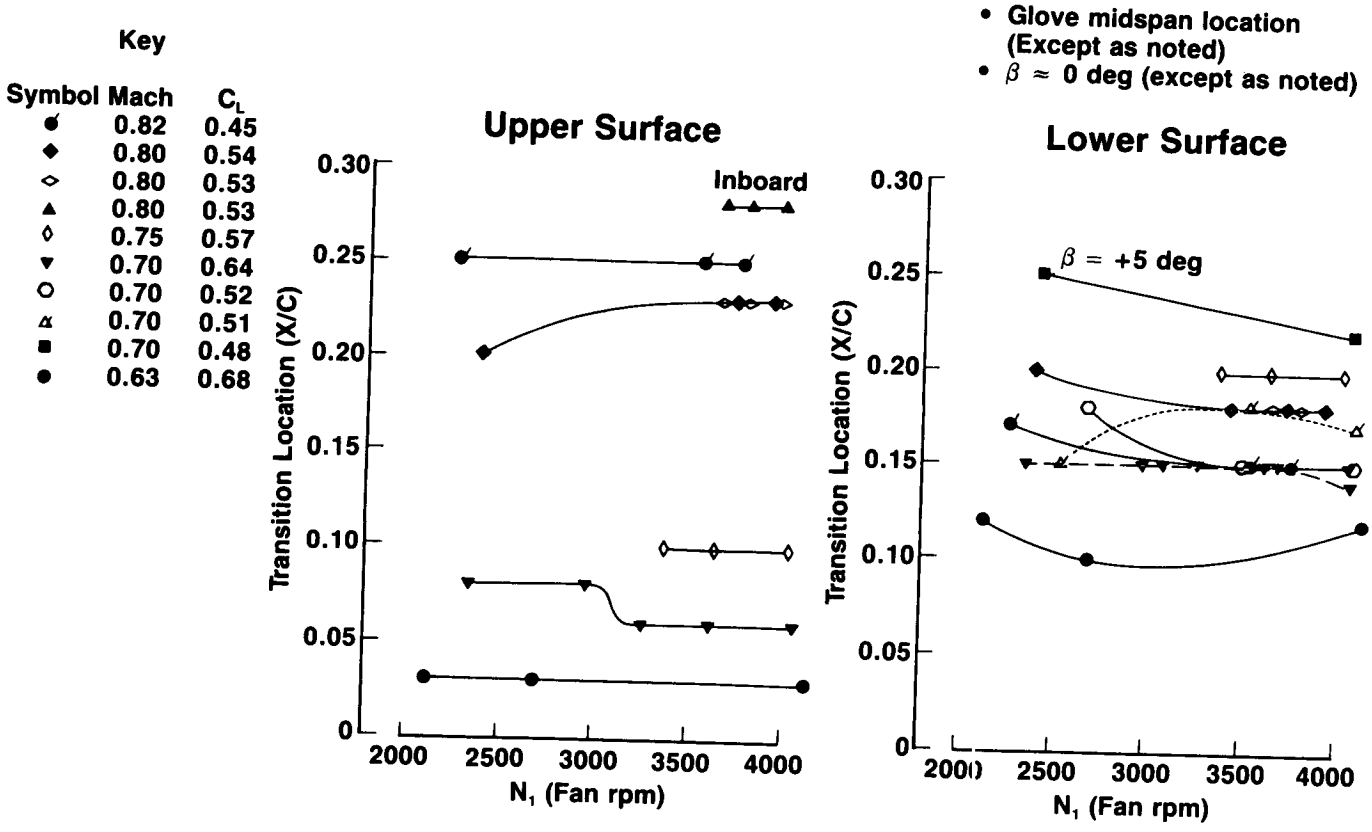

Figure 18

BOUNDARY-LAYER STABILITY ANALYSIS INPUT DATA

The 757 NLF glove provides a new source for empirical calibration of boundary-layer transition methods. Transition prediction methods based on linear boundary layer stability theory are currently the most widely used. Therefore, linear boundary-layer stability analysis was applied to twenty-one 757 flight data cases. The first step in the analysis of a given case was to generate the boundary-layer data, which consist of the velocity and temperature profiles. Figure 19 shows a typical set of flight data from which input data to the boundary-layer code (which was a Boeing infinite yawed wing compressible boundary-layer program) was generated. This flight data consisted of: 1) the isobar pattern, based on measured pressures at the inboard and outboard locations of the glove, together with guidance from the isobars predicted by the transonic analysis code; 2) the transition location, based on the hot film data; and 3) the pressure distribution at the chosen spanwise analysis station, interpolated from the measured inboard and outboard pressures in conjunction with the isobar pattern. For most cases, WBL 308.5 was the chosen analysis station. For the upper surface, this was usually the location of greatest laminar flow extent. It also was close to the inboard pressure measurement station, which minimized interpolation uncertainties.

The sample isobars shown in Figure 19 are typical of many of the upper surface cases analyzed. It can be seen that the isobar sweep in the leading edge region is much lower than that aft of 10% chord. Because of this, two separate infinite yawed wing analyses were made, each with a sweep angle representative of one of the two regions. The two solutions were then "patched" together in the vicinity of 10% chord.

- **Infinite Yawed Wing Boundary–Layer Analysis**
- **Upper Surface; WBL 308.5**
- **Flight 3, Condition 16 (Outbd Cp)**
- **Flight 2, Condition 233 (Inbd Cp)**
- **$M\infty$ = 0.804, Alt = 40,483 ft**
- **Re_c = 25.5 x 10^6**

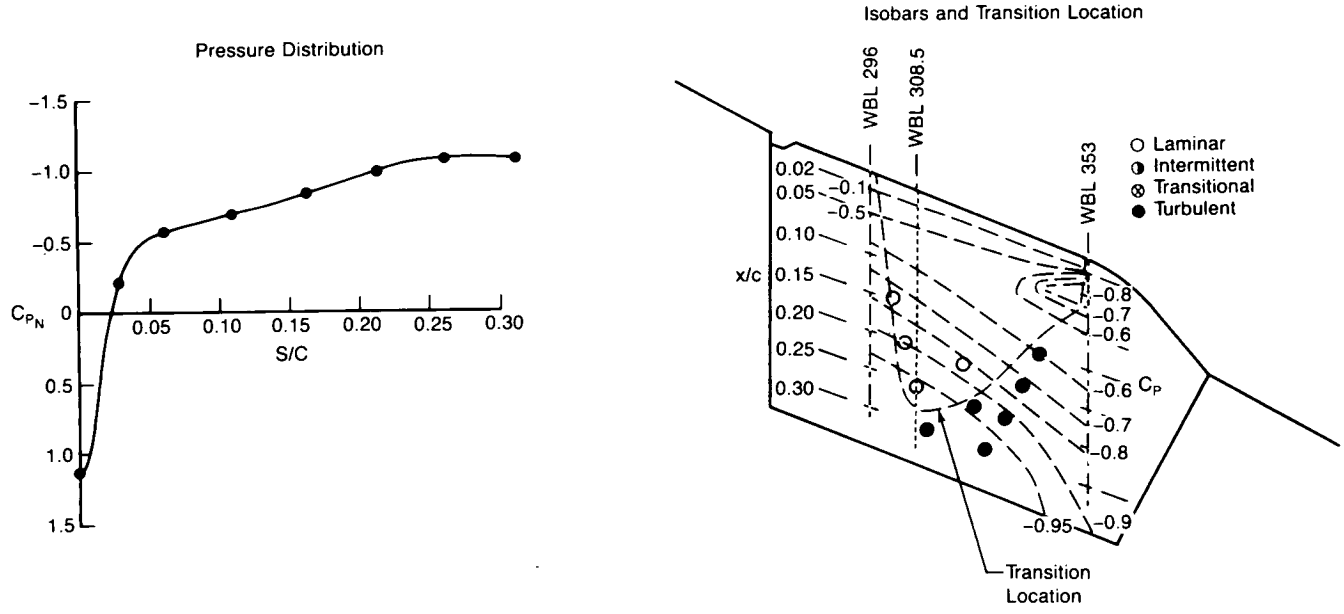

Figure 19

BOUNDARY LAYER STABILITY RESULTS

The calculated velocity and temperature profiles served as input data to the Boeing stability code (a modified version of the Mack code). This program solves the boundary-layer stability equations for three-dimensional, linearized, parallel flow in the spatial mode. For each flight condition both Tollmien-Schlichting (T-S) and cross flow (C-F) instabilities were analyzed. T-S amplification factors (NTS) were determined by keeping wave angle and frequency fixed. For crossflow amplification factors (NCF) the frequency was kept fixed at zero and the wave angle varied in accordance with the irrotationality condition (Ref. 5) for a fixed spanwise wave number component. A range of wave numbers was then analyzed to obtain the envelope of C-F disturbances. Sample results for these disturbance growths are shown in Figure 20. These results were then used to plot a trajectory curve on the NTS versus NCF plane, as shown.

The desired result is the N-factor combination at the measured transition location, indicated by the band near the end of the trajectory curve, the ends of which represent the location of the last laminar and first turbulent hot films. The figure also includes the F-111 transition data band, calculated in a previous study by applying the same method to flight data obtained by NASA on an NLF glove on the F-111 airplane (Ref. 6). This F-111 data band is the transition criterion that has been used at Boeing for the last several years.

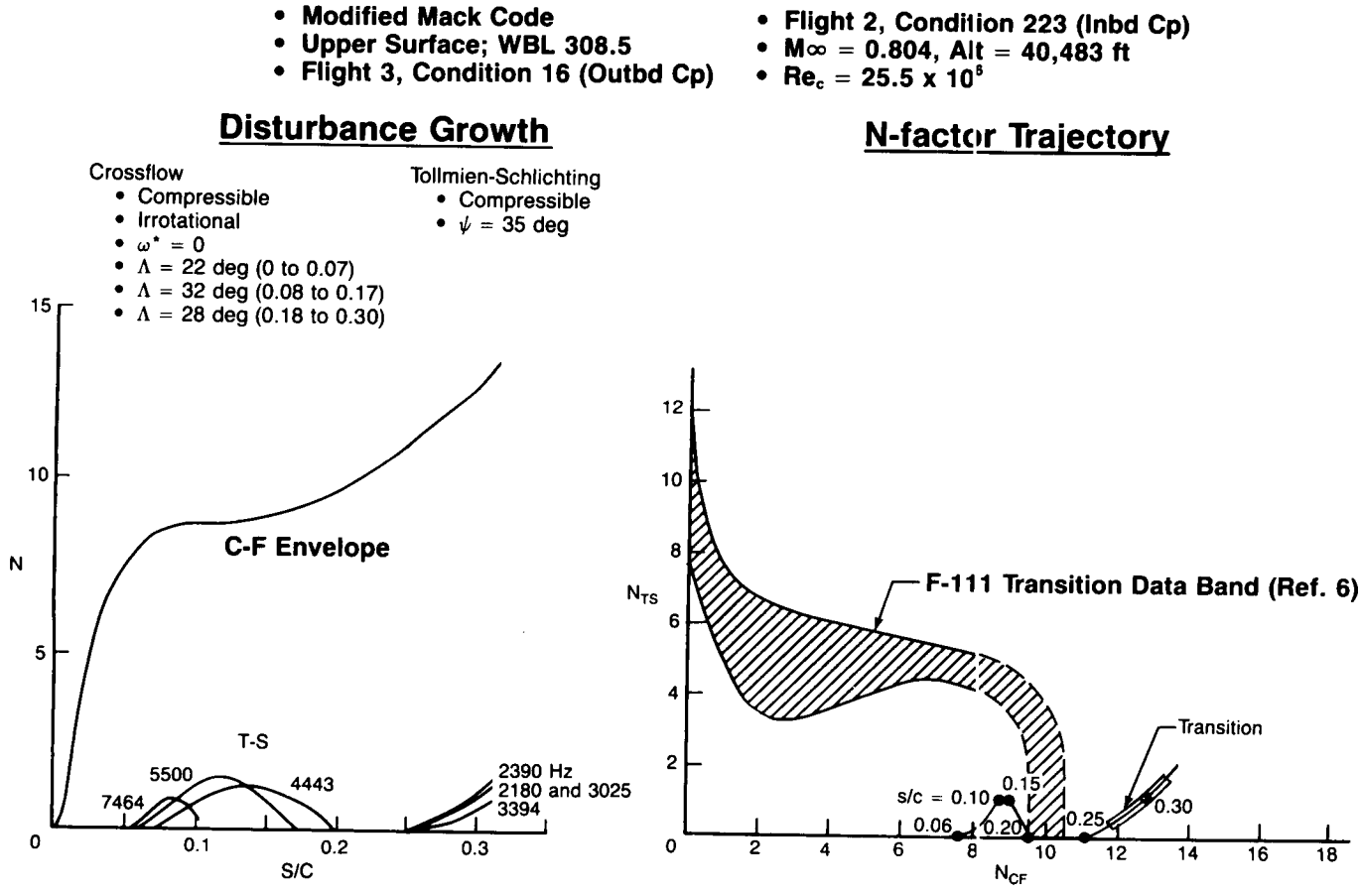

Figure 20

TOLLMIEN-SCHLICHTING TRANSITION N-FACTOR VERSUS CROSS-FLOW TRANSITION N-FACTOR

From the accumulated flight test data, a total of twenty-one cases were analyzed by the stability code. The final results, showing the values of NCF and NTS at transition (based on the middle of the transition uncertainty band), were all combined on a single plot, shown in Figure 21. Also included are the points from the previous F-111 calculations, which tend to fall in a different region of the diagram. The F-111 results had not provided any guidance in the low NTS, high NCF region of the diagram. Since this is where the bulk of the 757 data falls, the two sets of data complement each other. In the region of overlap between the two sets of data, there is fairly good agreement between the results. A band enclosing all of the F-111 data points and most of the 757 points provides a new transition criterion. Two of the 757 points below the band were not included because the degree of uncertainty in the measured pressures was higher for these cases than for the other cases. The 757 point above the band was not included simply because it lies outside of the region where the rest of the data lies. Excluding it tends to make the band more conservative.

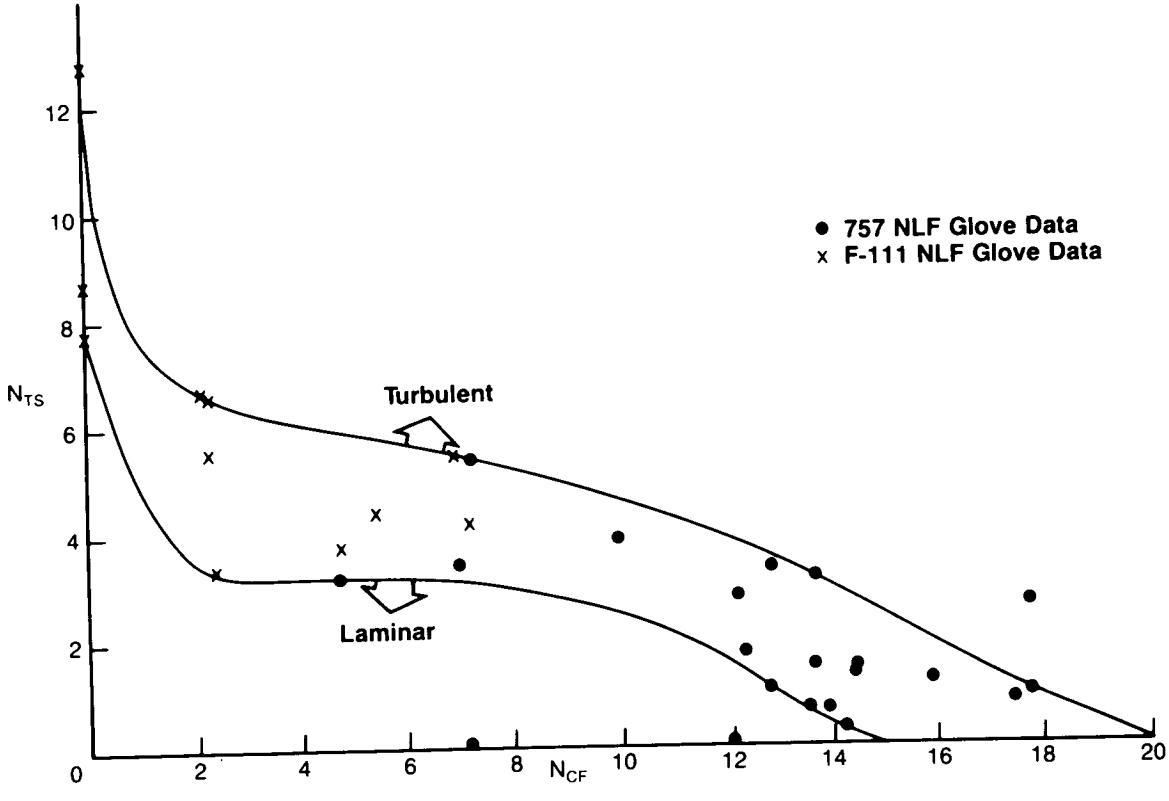

Figure 21

SUMMARY OF RESULTS

As a result of the 757 wing noise survey and NLF glove flight test, there now exists a large data base of near-field inflight noise measurements on the wing of a commercial transport with wing-mounted high-bypass-ratio engines. The data is for a wide range of airplane Mach numbers and altitudes and engine power settings. The data shows that aerodynamic noise is the dominant noise source on the upper surface and engine noise is the dominant noise source on the lower surface. At cruise, (M = 0.8, 39,000 ft) the upper surface OASPLs are 115 dB to 130 dB and the lower surface OASPLs are 120 to 140 dB.

The transition and noise measurements on the NLF glove show that there is no apparent effect of engine noise on the upper surface transition location. On the lower surface, the transition location moved forward 2% to 3% chord at most conditions from the engine's low-power setting to the high-power settings. Since the effect of noise on the extent of laminar flow is dependent upon the particular wing design, the lower surface noise effect may be larger for other wing designs.

A boundary layer stability analysis of 21 of the 757 flight data cases showed that cross-flow disturbances were the dominant cause of transition at most flight conditions. The results of this analysis provide additional calibration data for linear stability-based transition prediction methods. (Figure 22).

- **Wing noise environment**
  - **First large data base of near-field inflight noise measurements**
  - **On upper surface**
    - **Aerodynamic noise is the dominant source**
    - **OASPLs at cruise are 115 dB to 130 dB**
  - **On lower surface**
    - **Engine noise is the dominant source**
    - **OASPLs at cruise are 120 dB to 140 dB**
- **Effect of engine noise on transition location**
  - **No effect on upper surface**
  - **Small effect on lower surface (2% to 3% chord)**
  - **Lower surface effect may be larger for other wing designs**
- **Boundary layer stability analysis**
  - **Cross-flow disturbances were dominant cause of transition at most flight conditions**
  - **Analysis of 21 757 flight cases provides additional calibration data for transition prediction**

Figure 22

REFERENCES

1. "Boeing Commercial Airplane Company: Flight Survey of the 757 Wing Noise Field and Its Effects on Laminar Boundary Layer Transition," Volume I—Program Description and Data Analysis, NASA CR 178216, March 1987.

2. "Boeing Commercial Airplane Company: Flight Survey of the 757 Wing Noise Field and Its Effects on Laminar Boundary Layer Transition," Volume II—Data Compilation, NASA CR 178217, March 1987.

3. Smith, F. and Higton, D. J., "Flight Test on King Cobra, FZ.440 To Investigate the Practical Requirements for the Achievement of Low Profile Drag Coefficients on a Low Drag Airfoil," R&M No. 2375, H.M.S.O., London, 1950.

4. Tibbets, J. G., "Near Field Noise Prediction for Aircraft in Cruising Flight—Methods Manual," NASA CR 159105, August 1979.

5. Mack, L. M., "On the Stability of the Boundary Layer on a Transonic Swept Wing," AIAA Paper No. 79-0264, 1979.

6. Runyan, L. J., Navran, B. H., and Rozendaal, R. A., F-111 Natural Laminar Flow Glove Flight Test Data Analysis and Boundary Layer Stability Analysis," NASA CR-166051, January 1984.